High-frequency photoacoustic imaging of erythrocyte aggregation and oxygen saturation: probing hemodynamic relations under pulsatile blood flow

Tae-Hoon Bok, Eno Hysi, Michael C. Kolios[*]

Department of Physics, Ryerson University, 350 Victoria Street, Toronto, ON Canada M5B 2K3;
mkolios@ryerson.ca

ABSTRACT

In this paper, we investigate the feasibility of high-frequency photoacoustic (PA) imaging to study the shear rate dependent relationship between red blood cell (RBC) aggregation and oxygen saturation (SO_2) in a simulated blood flow system. The PA signal amplitude increased during the formation of aggregates and cyclically varied at intervals corresponding to the beat rate (30, 60, 120, 180 and 240 bpm) for all optical wavelengths of illumination (750 and 850 nm).The SO_2 also cyclically varied in phase with the PA signal amplitude for all beat rates. In addition, the mean blood flow velocity cyclically varied at the same interval of beat rate, and the shear rate (i.e. the radial gradient of flow velocity) also cyclically varied. On the other hand, the phase of the cyclic variation in the shear rate was reversed compared to that in the PA signal amplitude. This study indicates that RBC aggregation induced by periodic changes in the shear rate can be correlated with the SO_2 under pulsatile blood flow. Furthermore, PA imaging of flowing blood may be capable of providing a new biomarker for the clinical application in terms of monitoring blood viscosity, oxygen delivery and their correlation.

Keywords: Red blood cell aggregation, Oxygen Saturation, Shear rate, Pulsatile blood flow

1. INTRODUCTION

Red blood cell (RBCs) become aggregated when blood is exposed to stasis or very low shear rate conditions. RBC aggregation is promoted in various pathologies such as deep vein thrombosis, diabetes or a stoke [1-3], and is a dominant factor in blood viscosity which affects blood flow dynamics, vascular resistance and tissue perfusion [4]. Approaches that have been proposed for the measurement of RBC aggregation include measuring the erythrocyte sedimentation rate [5], low shear viscometry [6], ultrasound (US) imaging [7] and analysis of light transmission or reflection of RBC suspensions [8]. Among these methods, US imaging warrants special consideration as the only non-invasive assessment of RBC aggregation [7,9,10]. However, most studies of US imaging have focused on imaging the formation/disorganization of RBC aggregates in terms of their effect on the hemodynamic properties of blood. In other words, US imaging simply provides information on the RBC aggregate size, despite the fact that the RBC's fundamental role is the oxygen delivery to tissues.

The transport and delivery of oxygen is governed by the blood oxygen saturation (SO_2) [11]. The clinical significance of the SO_2 has been already widely reported [12,13]. For the measurement of the SO_2, traditional methods such as optical spectroscopy have been employed [14,15] but they are limited by the penetration depth of light and lack of spatial resolution. During the past decade, new SO_2 measurement techniques have been proposed through advances in photoacoustic (PA) imaging [16-19]. However, these previous studies have focused on the SO_2 measurement in micron-diameter vessels (predominantly arterioles and capillaries) without considering hemodydnamic and/or hemorheological effects such as RBC aggregation.

RBC aggregation and the SO_2 are intrinsically related phenomena linking structural and functional aspects of RBCs, respectively. Therefore, the relation between RBC aggregation and the SO_2 may provide a new biomarker for disorders where aggregation becomes pathological. According to Tateishi et al. [20,21], the diffusion of oxygen from RBC is inhibited when RBCs aggregate and when the cell-free plasma layer surrounding the aggregate is thickened. However, in their studies they showed the correlation between the SO_2 and RBC aggregation induced by Dextran T-70, not by the

---

[*] mkolios@ryerson.ca

natural hemodynamic behavior of flowing blood. In the previous studies by our group [22,23], the PA measurement of Dextran induced RBC aggregation and the SO_2 was preliminarily conducted under the static conditions of blood. For the advanced clinical applicability of PA imaging of blood, the relationship between RBC aggregation and the SO_2 should be investigated simultaneously under naturally varying hemodynamic conditions due to pulsatile flow. It is known that such pulsatile flow will create time varying shear rates in blood vessels thereby changing the dynamics of the formation of RBC aggregates.

In the current paper, high-frequency PA imaging is proposed to simultaneously assess RBC aggregation and the SO_2 under pulsatile blood flow at the beat rate from 30 to 240 bpm within a flow phantom. The flowing blood was imaged at two optical illumination wavelengths in order to estimate the SO_2 and to acquire the PA signal amplitude from blood using a high-frequency PA system. The Doppler flow velocity was measured, and the radial shear rate was estimated by the blood flow velocity in order to interpret the relation between RBC aggregation, the SO_2 and the shear rate.

2. MATERIALS AND METHODS

2.1 Blood source

Ethics approval was granted by the Research Ethics Boards of Ryerson University and the Canadian Blood Services. All experiments were conducted using whole blood units donated by healthy volunteers recruited by the Canadian Blood Services' Network Center for Applied Development (Vancouver, BC, Canada). Whole blood units from three volunteers were used in order to ensure the repeatability of experimental results.

2.2 Blood flow and PA imaging system

A blood flow system was configured by a peristaltic pump (MasterFlex, Cole-Parmer, Montreal, QC, Canada), a silicone tube, a triangle beaker, and a 2-mm-diameter flow phantom made from porcine skin gelatin (Sigma Aldrich, Oakville, ON, Canada) at a concentration of 15% wt/vol in degassed water. The silicone tube was connected to the flow phantom for circulating blood flow, and the beaker was used as a blood vessel and a reservoir (Fig. 1). The pulsatile flow at beat rates from 30 to 240 bpm were generated within the phantom by the peristaltic pump.

Flowing blood was imaged at 20 frame per second by a VevoLAZR (FUJIFILM VisualSonics, Toronto, ON, Canada) system equipped with a 40 MHz linear-array probe. An Nd:YAG pulsed laser (20 Hz, 6ns pulse width, 30 mJ/pulse) was operated at two optical wavelengths (750 and 850 nm) in order to estimate the SO_2 by the computing the ratio of oxygenated hemoglobin to the total hemoglobin assessed. PA measurements were performed for three blood samples, five beat rates, and two wavelengths.
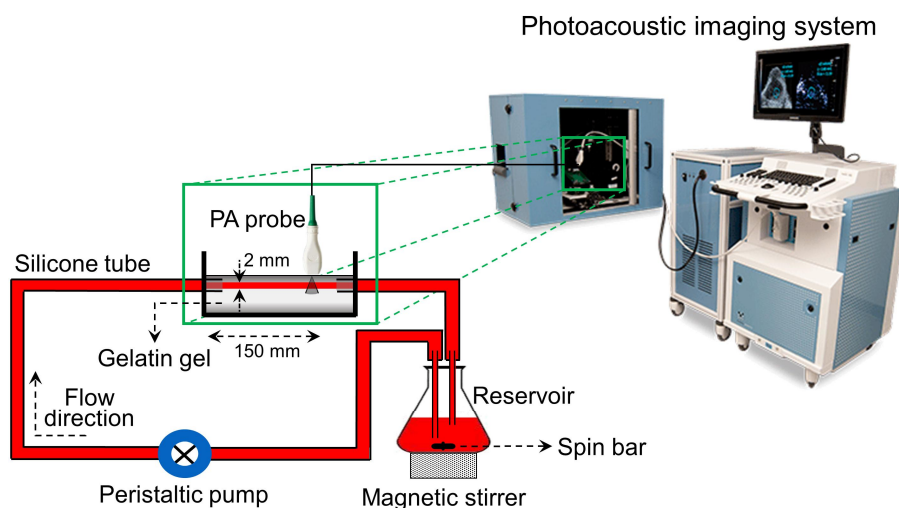

Figure 1. Experimental set-up of blood flow and photoacoustic imaging system

2.3 Simultaneous assessment of RBC aggregation and the SO$_2$ depending on the blood flow velocity

The PA signal amplitudes from RBC aggregates can be approximated as the PA signal amplitude from a sphere (P_s) as described by [24].

$$p_s(\hat{\tau}) = \frac{i\mu_a \beta F v_s^2 a}{2\pi C_p r} \int_{-\infty}^{\infty} \frac{\left[\sin\hat{q} - \hat{q}\cos\hat{q}\right]e^{-i\hat{q}\hat{\tau}}}{\hat{q}^2\left[(1-\hat{\rho})(\sin\hat{q}/\hat{q}) - \cos\hat{q} + i\hat{q}\hat{v}\sin\hat{q}\right]} d\hat{q} \tag{1}$$

where μ_a is the optical absorption coefficient, β is the isobaric thermal expansion coefficient, F is the optical fluence of the excitation light, v_s is the sound speed in the absorber, a is the radius of spherical absorber, C_p is the heat capacity per unit mass, r is the distance between the absorber and the ultrasonic detector, $\hat{q}$ is defined as $\hat{q} = \omega a/v_s$ where ω is the modulation frequency of the optical beam, $\hat{\tau}$ is the dimensionless retarded time from the edge of the sphere defined as $\hat{\tau} = (v_s/a)[t - (r-a)/v_f]$ where v_f is the sound speed in the surrounding fluid medium, $\hat{\rho} = \rho_s/\rho_f$ and $\hat{v} = v_s/v_f$ are the ratios of density and the sound speed, respectively, where ρ_s and ρ_f are the density of the absorber and the surrounding fluid medium, respectively. The PA signal amplitudes from aggregating blood is mainly governed by the radius of uniformly irradiated sphere (a) which is related to the aggregate size. Hence, the formation of RBC aggregation can be assessed by the changes in the PA signal amplitude.

The SO$_2$ was estimated by assuming that oxygenated (HbO) and deoxygenated (Hb) hemoglobin were the dominant absorbers at the two optical illumination wavelengths λ_1 and λ_2, and was computed by [16]

$$\text{SO}_2 = \frac{[\text{HbO}]}{[\text{HbO}]+[\text{Hb}]} = \frac{\mu_a^{\lambda_2}\varepsilon_{\text{Hb}}^{\lambda_1} - \mu_a^{\lambda_1}\varepsilon_{\text{Hb}}^{\lambda_2}}{\mu_a^{\lambda_1}(\varepsilon_{\text{HbO}}^{\lambda_2} - \varepsilon_{\text{Hb}}^{\lambda_2}) - \mu_a^{\lambda_2}(\varepsilon_{\text{HbO}}^{\lambda_1} - \varepsilon_{\text{Hb}}^{\lambda_1})} \tag{2}$$

where [HbO] and [Hb] are the molar concentrations of HbO and Hb, respectively; μ_a is the absorption coefficient and is equal to $P/(\Gamma \cdot F)$ where P is the detected PA pressure, Γ is the Gruneisen parameter, so that P is used instead of μ_a in this study. It is assumed that Γ and F are constant; and ε_{HbO} and ε_{Hb} are the known molar extinction coefficients of HbO and Hb, respectively.

In order to quantify the variation of the measurement parameters, the variation indices of the PA signal amplitude (VI$_{\text{PA}}$) and SO$_2$ (VI$_{\text{SO}}$) were computed by

$$\text{VI}_{\text{PA}} = \frac{1}{N}\sum_{n=1}^{N} \frac{\text{PA}_{\text{amp, max}} - \text{PA}_{\text{amp, min}}}{\text{PA}_{\text{amp, mean}}}\Bigg|_{T_n}$$
$$\text{VI}_{\text{SO}} = \frac{1}{N}\sum_{n=1}^{N} \frac{\text{SO}_{2,\,\text{max}} - \text{SO}_{2,\,\text{min}}}{\text{SO}_{2,\,\text{mean}}}\Bigg|_{T_n} \tag{3}$$

where N is the number of cycles, T_n is the order of cycle, PA$_{\text{amp}}$ is the PA signal amplitude, and the subscripts max, min and mean indicate the maximum, minimum and average values, respectively.

Ideally, the blood flow velocity should be simultaneously measured with the PA images in order to interpret the relation between RBC aggregation, the SO$_2$ and the shear rate which is the radial gradient of the flow velocity. The PA system, however, was limited in the ability to measure PA signals and blood flow velocities simultaneously. In lieu of that, the Doppler blood flow velocity was separately measured by the PA system. The flow velocity was manually synchronized with the vessel diameter since the vessel expands and contracts during systole and diastole, respectively [25]. The mean shear rate was estimated by assuming that the radial profile of flow velocity was linear, and the peak velocity of the radial profile was the mean blood flow velocity measured by the Doppler power at each time point. It is worth noting that the radial profile of flow velocity for steady flow is parabolic, and that for the pulsatile flow is dependent on the phase of flow. This makes the determination of the radial shear rate a difficult quantity to assess. However, the mean shear rate can be approximated by the aforementioned method. The standard deviation of the shear rate was computed considering the cyclic variation in the blood flow velocity.

3. RESULT AND DISCUSSION

The PA signal amplitudes at two wavelengths 750 and 850 nm varied periodically for all beat rates, as shown in Fig. 2a-e. The source of the PA signal was the RBCs and their aggregation as shown from our previous work [22,23], so the cyclic variation in the PA signal amplitude represents cyclical changes in RBC aggregation/disaggregation. The shear rate (determined by the radial gradient of the laminar flow velocity in a cylindrical tube) is governed by the blood flow velocity suggesting that the shear rate increases as the blood flow velocity increases. Hence, the mean shear rate also varied periodically with time as marked in green lines in Fig. 2. Even though the cyclic variations in RBC aggregation/disaggregation and shear rate were estimated by the variations in the PA signal amplitude and the blood flow velocity, the phases of cyclic variations were opposite each other at all the beat rates. The out-of-phase nature was due to the relation between RBC aggregation and shear rate, i.e. the maximal amount of RBC aggregation occurs when the shear rate is at a minimum. The out-of-phase relationship between RBC aggregation and the shear rate was consistent with a previous study using high-frequency ultrasound [26].

The SO_2 also varied periodically depending for all beat rates, as shown in Fig. 2f-j. The phase of cyclic variation in the SO_2 was the same as the variation in the PA signal amplitude. This observation suggested that RBC aggregation enhanced the SO_2. According to Tateishi et al. [20,21], the oxygen release is inhibited by RBC aggregation, so that the SO_2 increases and decreases during RBC aggregation and disaggregation, respectively. Hence, the phases of cyclic variation in the SO2 and the shear rate was opposite each other.
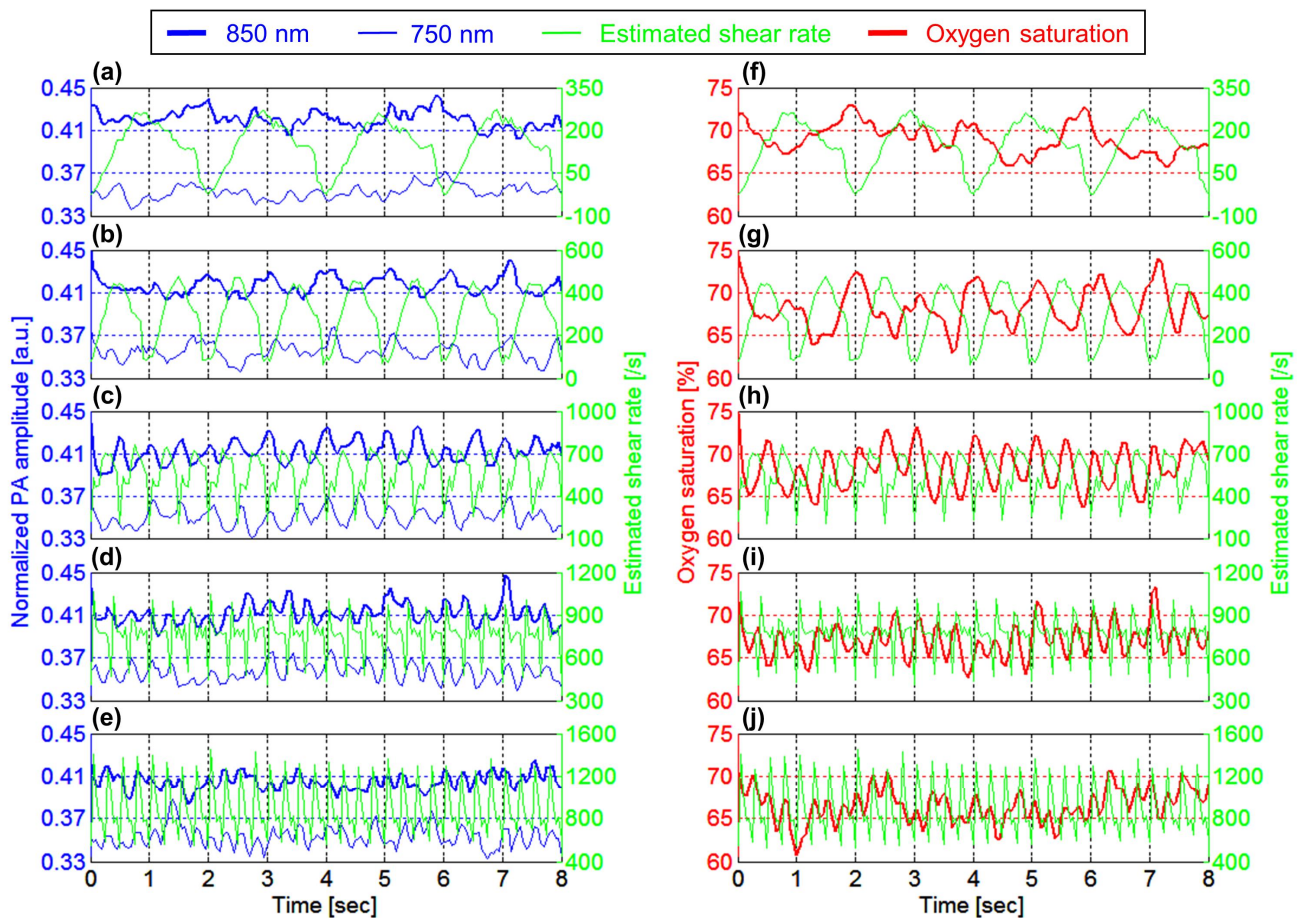

Figure 2. Cyclic variation in photoacoustic (PA) amplitude (a to e) and oxygen saturation (SO_2) (f to j) depending on the estimated mean shear rate at 30, 60, 120, 180 and 240 bpm of beat rates. The thick and thin blue lines indicate 850 and 750 nm of optical wavelength, respectively, the green line indicates the estimated mean shear rate, and the red line indicates the SO_2.

The mean shear rate increased with the beat rate since the mean blood flow velocity increases with the beat rate. This is shown in Fig. 3a. The variation indices VI_{PA} and VI_{SO} characterize the variability of the PA signal amplitude and the SO_2, respectively (Eq. 3). The PA signal amplitude is determined by RBCs and their aggregation, and the blood flow velocity determines the shear rate through its radial gradient. Hence, the VI_{PA} can be related to the variability of RBC aggregation and shear rate, respectively. The results presented in Fig. 3b show that, as the mean shear rate increased, the VI_{PA} and the VI_{SO} decreased.

The large variation in shear rate results in large variations in the RBC aggregation and the SO_2. We expected that the variability in the PA signal amplitude (as well as the SO_2) should increase as the variability in the shear rate increases. However, the variation in RBC aggregation (as assessed by the VI_{PA} at 750 and 850 nm) and the SO_2 (VI_{SO}) decreased as the variation in the shear rate increased (as assessed by the error bar). This apparently conflicting result can be explained by the increase in the mean shear rate. The mean shear rate increased with the beat rate, since the mean blood flow velocity increased with the beat rate. Even though the variability in the shear rate (assessed by the error bar) increased with the beat rate, the mean shear rate also increased, inhibiting RBC aggregation. Since non-aggregated RBCs would release oxygen more freely than aggregated RBCs, the SO_2 decreased as the shear rate increased.
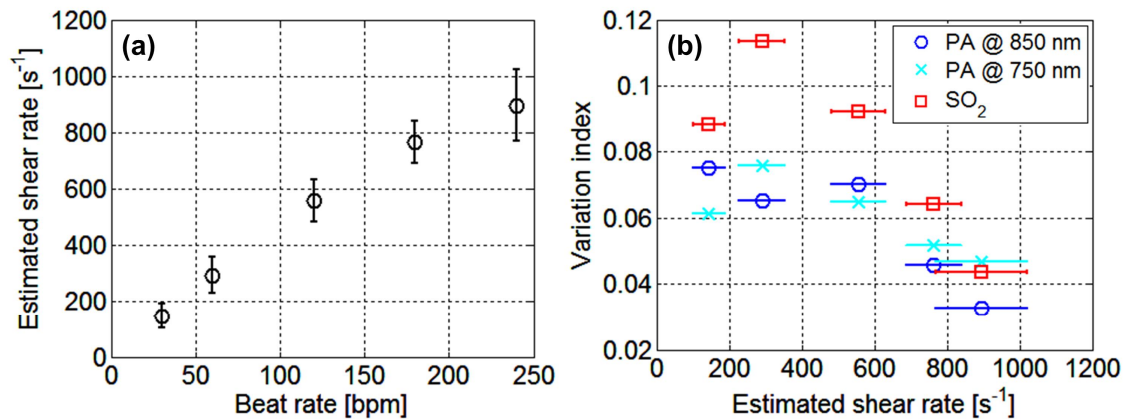

Figure 3. (a) The estimated mean shear rate vs. beat rate. (b) Variation indices of PA signal amplitude at 850 (blue circle) and 750 (cyan x) nm and the oxygen saturation (red square) vs. estimated shear rate. The error bar indicates the standard deviation of the estimated shear rate for the cyclic variation in the blood flow velocity.

4. CONCLUSION

The PA signal amplitudes at 750 and 850 nm and the mean blood flow velocity were measured by high-frequency PA imaging under pulsatile blood flow at the beat rate of 30, 60, 120, 180 and 240 bpm. They were determinants of RBC aggregation and the shear rate, respectively. The SO_2 was computed by the two optical wavelength method from the PA signal amplitude. The PA signal amplitudes and the SO_2 varied periodically as a function of the beat rate, and they were in phase each other, and out of phase with the estimated mean shear rate. Since the PA signal amplitudes and the blood flow velocity are directly influenced by RBC aggregation and the shear rate, respectively, RBC aggregation and the SO_2 were in phase each other, and out of phase with the shear rate. These findings suggest that PA assessment of RBC aggregation in various circulatory disorders could be achieved through imaging of accessible human blood vessels such as the radial artery or vein. This study is a preliminary investigation that opens new avenues towards understanding the relationship between RBC aggregation, SO_2 and hemodynamics in PA imaging.

REFERENCES

[1] Yu, F. T. H., Amstrong, J. K., Tripette, J., Meiselman, H. J. and Cloutier, G., "A local increase in red blood cell aggregation can trigger deep vein thrombosis: evidence based on quantitative cellular ultrasound imaging," J. Thromb. Haemost. 9, 481-488 (2011).

[2] Li, Q., Li, L. and Li, Y., "Enhanced RBC aggregation in type 2 diabetes patients," J. Clin. Lab. Anal. 00, 1-3 (2014).

[3] Bok, T., Kong, Q., Nam, K., Oh, Y. H., Kim, J. G., Lee, J. J., Choi, J. C. and Paeng, D.,"A pilot study of blood echogenicity from the radial artery and the carotid artery of stroke patients," in *Proceedings of IEEE International Ultrasonics Symposium*, 2364-2367 (2012).

[4] Baskurt, O. K. and Meiselman, H. J., "Erythrocyte aggregation: Basic aspects and clinical importance," Clin. Hemorheol. Microcirc. 53, 23-37 (2013).

[5] Erikssen, G., Liestøl, K., Bjørnholt, J. V., Stormorken, H., Thaulow, E. and Erikssen, J., "Erythrocyte sedimentation rate: a possible marker of atherosclerosis and a strong predictor of coronary heart disease mortality," Eur. Heart J. 21, 1614-1620 (2000).

[6] Brooks, D. E., Goodwin, J. W. and Seaman, G. V. F., "Rheology of erythrocyte suspensions: Electrostatic factors in the dextranmediated aggregation of erythrocytes," Biorheology 11, 69-76 (1974).

[7] Cloutier, G. and Qin, Z., "Ultrasound backscattering from non-aggregating and aggregating erythrocytes - a review," Biorheology 34, 443-470 (1997).

[8] Hardeman, M. R., Dobbe, J. G. G. and Ince, C., "The laser-assisted optical rotational cell analyzer (LORCA) as red blood cell aggregometer," Clin. Hemorheol. Microcirc. 25, 1-11 (2001).

[9] Li, Y., Bok, T., Yang, J., Choi,M. J. and Paeng, D., "The acute effects of smoking on the cyclic variations in blood echogenicity of carotid artery," Ultrasound Med. Biol. 37, 513-521 (2011).

[10] Paeng, D., Nam, K. and Shung, K. K., "Cyclic and radial variation of the echogenicity of blood in human carotid arteries observed by harmonic imaging," Ultrasound Med. Biol. 36, 1118-1124 (2010).

[11] Walley, K. R., "Use of central venous oxygen saturation to guide therapy," Am. J. Respir. Crit. Care Med. 184, 514-520 (2011).

[12] Pope, J. V., Jones, A. E., Gaieski, D. F., Arnold, R. C., Trzeciak, S. and Shapiro, N. I., "Multicenter study of central venous oxygen saturation ($ScvO_2$) as a predictor of mortality in patients with sepsis," Ann. Emerg. Med. 55, 40-46.e1 (2010).

[13] Jones, A. E., Shapiro, N. I., Trzeciak, S., Arnold, R. C., Claremont, H. A. and Kline, J. A., "Lactate clearance vs central venous oxygen saturation as goals of early sepsis therapy: A randomized clinical trial," J. Am. Med. Assoc. 303, 739-746 (2010).

[14] Chance, B., Borer, E., Evans, A., Holtom, G., Kent, J., Maris, M., McCully, K., Northrop, J. and Shinkwin, M., "Optical and nuclear magnetic resonance studies of hypoxia in human tissue and tumors," Ann. N. Y. Acad. Sci. 551, 1-16 (1988).

[15] Liu, H., Boas, D. A., Zhang, Y., Yodh, A. G. and Chance, B., "Determination of optical properties and blood oxygenation in tissue using continuous NIR light," Phys. Med. Biol. 40, 1983 (1995).

[16] Wang, X., Xie, X., Ku, G., Wang, L. V. and Stoica, G., "Noninvasive imaging of hemoglobin concentration and oxygenation in the rat brain using high-resolution photoacoustic tomography," J. Biomed. Opt. 11, 024015-1-024015-9 (2006).

[17] Wang, L., Maslov, K. and Wang, L. V., "Single-cell label-free photoacoustic flowoxigraphy in vivo," Proc. Natl. Acad. Sci. USA 110, 5759-5764 (2013).

[18] Zhang, H. F., Maslov, K., Sivaramakrishnan, M., Stoica, G. and Wang, L. V., "Imaging of hemoglobin oxygen saturation variations in single vessels in vivo using photoacoustic microscopy," Appl. Phys. Lett. 90, 053901-1-053901-3 (2007).

[19] Zhang, H. F., Maslov, K., Stoica, G. and Wang, L. V., "Functional photoacoustic microscopy for high-resolution and noninvasive in vivo imaging," Nat. Biotech. 24, 84-851 (2006).

[20] Tateishi, N., Suzuki, Y., Cicha, I. and Maeda, N., "O_2 release from erythrocytes flowing in a narrow O_2-permeable tube: effects of erythrocyte aggregation," Am. J. Physiol. - Heart Circul. Physiol. 281, H448-H456 (2001).

[21] Tateishi, N., Suzuki, Y., Shirai, M., Cicha, I. and Maeda, N., "Reduced oxygen release from erythrocytes by the acceleration-induced flow shift, observed in an oxygen-permeable narrow tube," J. Biomech. 35, 1241-1251 (2002).

[22] Hysi, E., Saha, R. K. and Kolios, M. C., "Photoacoustic ultrasound spectroscopy for assessing red blood cell aggregation and oxygenation," J. Biomed. Opt. 17, 125006-1-125006-10 (2012).

[23] Hysi, E., Saha, R. K. and Kolios, M. C., "On the use of photoacoustics to detect red blood cell aggregation," Biomed. Opt. Express 3, 2326-2338 (2012).

[24] Wang, L. V., [Photoacoustic Imaging and Spectroscopy], CRC Press, Boca Raton, 2-17 (2009).

[25] Eriksen, M., "Effect of pulsatile arterial diameter variations on blood flow estimated by Doppler ultrasound," Med. Biol. Eng. Comput. 30, 46-50 (1992).

[26] Bok, T., Li, Y., Nam, K., Choi, J. C. and Paeng, D., "Feasibility study of high-frequency ultrasonic blood imaging in the human radial artery," J. Med. Biol. Eng. 35, in press (2015).